



Giving the cells what they need when they need it: Biosensor-based feeding control

Romain Kinet¹  | Anne Richelle¹ | Michael Colle¹ | Didier Demaegd¹ |
 Moritz von Stosch¹ | Matthew Sanders¹ | Hannah Sehart² | Frank Delvigne²  |
 Philippe Goffin³

¹GSK, Rixensart, Belgium

²TERRA Teaching and Research Centre, Gembloux Agro-Bio Tech, University of Liège, Gembloux, Belgium

³Molecular and Cellular Biology, University of Brussels, Brussels, Belgium

Correspondence

Romain Kinet

Email: romain_kinet@hotmail.com

Present address

Moritz von Stosch, DataHow AG, Oerlikon, Switzerland.

Funding information

GlaxoSmithKline; Wagralim-Biowin

Abstract

“Giving the cells exactly what they need, when they need it” is the core idea behind the proposed bioprocess control strategy: operating bioprocess based on the physiological behavior of the microbial population rather than exclusive monitoring of environmental parameters. We are envisioning to achieve this through the use of genetically encoded biosensors combined with online flow cytometry (FCM) to obtain a time-dependent “physiological fingerprint” of the population. We developed a biosensor based on the *glnA* promoter (*glnAp*) and applied it for monitoring the nitrogen-related nutritional state of *Escherichia coli*. The functionality of the biosensor was demonstrated through multiple cultivation runs performed at various scales—from microplate to 20 L bioreactor. We also developed a fully automated bioreactor–FCM interface for on-line monitoring of the microbial population. Finally, we validated the proposed strategy by performing a fed-batch experiment where the biosensor signal is used as the actuator for a nitrogen feeding feedback control. This new generation of process control, —based on the specific needs of the cells, —opens the possibility of improving process development on a short timescale and therewith, the robustness and performance of fermentation processes.

KEYWORDS

biosensor, *Escherichia coli*, nitrogen starvation, online flow cytometry, process control

1 | INTRODUCTION

In the biopharmaceutical industry, the screening and selection of microbial strains for recombinant protein production are crucial steps in process development (Brondyk, 2009; Zeng et al., 2020). This choice is most often based on the comparison of phenotype attributes displayed by the different potential hosts. The most prominent phenotype attributes considered are the growth capacity of the host cell and its capacity to produce high amount of the recombinant protein of interest with the proper quality attributes (e.g., folding, [sequence] integrity, posttranslational modifications). While numerous host-specific factors (related to the genetic

background) can influence these phenotype attributes, culture conditions remain the main limiting factor in the acquisition of an optimal phenotype (Delvigne et al., 2014; Heins & Weuster-Botz, 2018).

Common sensors available in industrial bioreactors most often focus on the monitoring of a small number of so-called “process variables” (e.g., pH, OD, dissolved oxygen [DO] concentration, etc.). In the last two decades, more advanced analytical technologies (e.g., chromatography, spectrometry, spectroscopy) have attracted increasing interest for the monitoring of more complex physico-chemical parameters, specifically for the measurement of metabolites and cell concentrations (Esmonde-White et al., 2017; Mandenius &

Gustavsson, 2016; Ryder, 2018). While these techniques were initially not suitable for automated monitoring systems, due to limitations in data processing and analysis time, continuous advances in these fields are now paving the way toward tools with the capacity of measuring multiple metabolites and compounds of interest in situ and in real-time (Dietzsch et al., 2013). However, these tools only provide information on the global environment at the population level but are not suited for capturing the microenvironment surrounding and influencing the physiological state of each individual cell (Delvigne & Goffin, 2014; Lemoine et al., 2017; Richelle et al., 2020).

In this context, we developed a system enabling the real-time monitoring of the nutritional state of *Escherichia coli* at the single-cell level to specifically track the onset of nitrogen-limiting conditions. Nitrogen is one of the major substrate requirements for growth, and a driver of shifts in metabolism, together with carbon and energy sources. Therefore, nitrogen depletion is a phenomenon that can significantly influence the performance of a cell culture (Bhattacharya & Dubey, 1997; Thomsson et al., 2005; Tibocho-Bonilla et al., 2020; Xu et al., 2016).

In our system, the sensing module consists in a genetically encoded biosensor. We developed and validated a biosensor enabling the detection of the nitrogen starvation state of individual cells. Genetically encoded biosensors involve genetic circuits that can report (usually via the expression of a fluorescent protein) on the physiological state of cells or the presence or absence of metabolites of interest (Polizzi & Kontoravdi, 2015). Based on the development of a specific interface, the fluorescence generated by the biosensor during nitrogen-limiting conditions can be detected in real-time using flow cytometry (FCM) without sample preprocessing. This knowledge was used to implement a closed-loop fractionated feeding control, ensuring an appropriate nitrogen supply throughout the culture. The combination of a fluorescent biosensor with FCM analysis, enables monitoring at the population level while allowing the detection of specific phenotypes of interest at the single-cell level.

This work has been done in the context of the establishment of new technologies aiming at interfacing cell population with computers to better control the biological performances of the system. A lot of studies have already addressed the issue of cell-to-cell heterogeneity in gene expression based on the use of such interface (Benisch et al., 2023; Bertaux et al., 2022; Kumar et al., 2021). However, most of these studies have been focused on the use of optogenetics, that is, the use of light to actuate cell population based on light-sensitive gene circuits (Carrasco-López et al., 2020; Kumar & Khammash, 2022). The second caveat of most of the studies focused on interfacing cell population with computer is that most of the experiments are conducted in cultivation devices exhibiting performances that are below the ones offered by the bioreactors used in industry, that is, lack of oxygen transfer efficiency, no pH control, limitation to batch mode of production. This issue has already been recognized in the field of synthetic biology and efforts have been made for developing open systems for the more accurate characterization of gene circuits in cell populations, for example, eVOLVER (Wong et al., 2018) and Chi.Bio (Delvigne & Martinez, 2023;

Steel et al., 2020). However, even if these systems offer many possibilities in terms of online monitoring, there are still limited at the level of mixing and mass transfer performances. Accordingly, the aim of this work is to bridge this gap by showing that it is also possible to actuate cell populations in more realistic bioreactor set-up. Indeed, it is not straightforward to couple automated FCM to bioreactors operated in fed-batch mode conditions and particular attention will be paid to the technical details needed for achieving such operations.

2 | MATERIAL AND METHODS

2.1 | Design of a *glnAp*-based biosensor

A *glnAp*-based biosensor was constructed, which is made of the *glnAp* promoter from *E. coli* BLR (DE3) as an input module and Green Fluorescent Protein (GFP) mut3.1 with a C-terminal destabilization tag (ASV; Andersen et al., 1998) as an output module. The entire expression cassette contains (from 5' to 3', relative to the orientation of the GFPmut3.1 open reading frame): (i) a transcription terminator for insulation of the expression cassette, (ii) a 494 bp DNA sequence encompassing the intergenic sequence between genes *typA* and *glnA* from *E. coli* BLR (DE3) (Goffin & Dehottay, 2017), which contains both *glnAp1* and *glnAp2* promoters (nucleotides 3956519–3957012 in accession number CP020368), (iii) a ribosome binding site optimized for strong expression of the downstream gene(s) (RBS0034b), (iv) a codon-optimized gene encoding GFPmut3.1 fused to (v) a sequence encoding the RPAANDENYAASV amino acid sequence, which targets GFPmut3.1 for degradation (nucleotide sequence obtained from Andersen et al. (1998); degradation tag in bold), (vi) a 3'-UTR containing two stop codons in the frame of the GFPmut3.1 ORF, and one stop codon in every alternative frame, and (vii) a bidirectional transcription terminator for avoiding transcriptional interference with the downstream sequence. The full annotated sequence of the biosensor expression cassette is provided as Supporting Information S2: File 1. Practically, fragments of the expression cassette were assembled from synthetic genes (Genscript), synthetic gene fragments (IDT) and oligonucleotides (MilliporeSigma) in successive restriction/ligation cloning steps in plasmid pBeloBAC11, which contains a chloramphenicol resistance gene as a selection marker (New England Biolabs). The biosensor as a whole was designated *glnAp*-GFP-ASV. All construct steps were performed in *E. coli* DH10B, and the final plasmid containing the biosensor (pSC1001d-*glnAp*-0034b) was transformed into *E. coli* BLR (DE3) by electroporation. To provide a negative control for all experiments, the unmodified pBeloBAC11 plasmid was also transformed into *E. coli* BLR (DE3).

2.2 | Cultivation medium

All cultures were performed in a chemically defined medium (CDM) (see Supporting Information S1: Table 1 for detailed composition). This medium was adapted from media developed by Wang et al. (2005) and Babaeipour et al. (2007). It contains glucose as a carbon

source and essential mineral elements. Ammonium was used as the major nitrogen source. The medium was supplemented with isoleucine (1 g/L) because of *E. coli* BLR(DE3) auxotrophy (Goffin & Dehottay, 2017), and with chloramphenicol (15 µg/mL) as a selection agent.

2.3 | Offline biomass concentration measurement

When monitored offline, biomass concentration is expressed as optical density (OD). Absorbance measurements were performed at 650 nm using Genesis 10S UV-Vis spectrophotometer (Thermo Fisher Scientific).

2.4 | Biolector cultivation—Biosensor functional validation

Validation of the biosensor functionality at small scale was performed by cultivating the transformed *E. coli* strain in CDM with different initial NH₄Cl concentrations. Precultures were performed in shake flasks (60 mL CDM in 150 mL flasks maintained at 37°C under orbital shaking at 200 rpm). Once cells from the pre-culture had entered the exponential growth phase, each well of a 48-well plate (FlowerPlate, M2P-lab) was inoculated with a defined volume of the preculture, such as to achieve an initial biomass concentration equivalent to an OD of 0.022 (650 nm). The following initial NH₄Cl concentrations were tested: 0.12, 0.3, 0.6, and 3 g/L. Cultures were performed in a Biolector device (M2P-lab) at 37°C, with a relative humidity of 85%, under constant agitation at 1500 rpm (3 mm shaking diameter, orbital), and with a working volume of 800 µL. Biomass concentration was monitored via scattered light intensity (620 nm). The intensity of the green fluorescence emitted by the cells was also recorded online. An excitation light at 488 nm was used for the characterization of GFP production, the fluorescence being collected using a 520 nm optical filter.

2.5 | Microfluidic cultivations

Cells were grown in microfluidic chips generously supplied by Alexander Grünberger's lab (ref. 24 W, chamber dimensions: 80 µm × 80 µm × ~850 nm; Täuber et al., 2020). Cultivation took place in CDM at a constant temperature of 37°C. The chambers were inoculated with 10–20 cells by flushing the device with a cell suspension (OD between 0.4 and 0.5). Three cultivation chambers were manually chosen for measuring the GFP fluorescence and the evolution of the number of cells with time. Cells were cultivated in CDM medium for 3.3 h before the conditions are switched to the same medium without ammonium. After 6 h under nitrogen-free conditions, cells were switched back to normal cultivation conditions. Microscopy images were taken using a Nikon Eclipse Ti2-E inverted automated epifluorescence microscope (Nikon Eclipse Ti2-E, Nikon

France), equipped with a DS-Qi2 camera (Nikon camera DSQi2, Nikon France), and a ×100 oil objective (CFI P-Apo DM Lambda 100× Oil (Ph3), Nikon France). GFP-3035D cube (excitation filter: 472/30 nm, dichroic mirror: 495 nm, emission filter: 520/35 nm, Nikon France) was utilized for GFP fluorescence measurement. Phase-contrast images were captured with an exposure time of 300 ms and an illuminator intensity of 30%. GFP images were recorded with an exposure time of 500 ms and an illuminator intensity of 2% (SOLA SE II; Lumencor). The acquisition of images, as well as the management of optical parameters and time-lapse settings, was conducted using the NIS-Elements Imaging Software (Nikon NIS Elements AR Software Package, Nikon France). GFP intensity was recorded each 20 min and the number of cells each 5 min.

2.6 | DasGip cultivation—In-process functionality validation

A preculture (60 mL CDM in 150 mL flasks maintained at 37°C under orbital shaking at 200 rpm) was inoculated with the transformed *E. coli* strain (Section 2.1) from a frozen seed. A 2 L glass bioreactor (DASGIP Parallel Bioreactor System, Eppendorf) containing 700 mL of CDM with a 150 mM initial ammonium concentration (sufficient to ensure supply during the entire batch phase) and 250 µL irradiated SAG471 antifoam was inoculated with a volume of preculture allowing to reach an initial biomass concentration equivalent to an OD (650 nm) of 0.022. Mechanical mixing was ensured by three TD6 Rushton impellers. The bioreactor was operated with the following regulations during batch phase: DO 20% saturation (regulated by stirring), pH 7 (regulated by NaOH 2.5 M), 30 NL/min sparged air, 10 NL/min sparged oxygen, 37°C. After glucose exhaustion, bioreactor operation was switched to glucose-limited DO-stat fed-batch fermentation: all regulations as in batch, except for DO and stirring speed. Mechanical mixing was maintained at 700 rpm and DO was regulated at 20% by the addition of concentrated feeding solution (glucose as carbon source, see Supporting Information S1: Table 2 for detailed composition). Briefly, the DO-stat strategy aims at controlling the substrate addition in the bioreactor based on the sharp change of DO as an indicator for feedback control (Lv et al., 2020; Seo et al., 1992). Upon the limiting substrate (i.e., glucose) is completely depleted, DO concentration tends to rapidly increase thus resulting in the automatic addition of the feeding solution. Subsequently, this substrate addition induces a decrease of the DO value which in turn results in the automatic stop of the feeding solution addition. PID controller was used to optimize the feeding flow rates and thus to maintain DO value as close as possible to the target value (i.e., 20% of saturation). Two feeding solutions were alternated, one was supplemented with NH₄Cl at 1.4 M while the other was nitrogen-free. Initially, the nitrogen-free feeding solution was used until the onset of nitrogen-limiting conditions. Once such conditions were observed (as detected through biosensor activation and confirmed by analytical technique), the solution supplemented

with nitrogen was implemented. Finally, the nitrogen-free solution was implemented again.

2.7 | 20 L-scale fermentations—Pilot-scale validation

Precultures (100 mL CDM in 250 mL flasks maintained at 37°C under orbital shaking at 200 rpm) were inoculated from a frozen seed. Stainless steel bioreactors (BioLafitte) containing 9 L of CDM with 3 mL irradiated SAG471 antifoam were inoculated with a volume of preculture allowing to reach an initial biomass concentration equivalent to an OD value of 0.0022 (650 nm). Mechanical mixing was ensured by three TD4 Rushton impellers. The bioreactors were operated with the following regulations during batch phase: DO 20% (regulated by stirring), pH 7 (regulated by NaOH 2.5 M), 20 NL/min sparged air, 0.5 bar overpressure, 37°C. Upon glucose exhaustion, bioreactor mode of operation was switched to glucose-limited DO-stat fed-batch fermentation. At this moment, all the control loops were set as for the batch phase, except for DO and stirring speed. Mechanical mixing was maintained at 700 rpm and DO was regulated at 20% by the addition of concentrated feed solution (glucose as carbon source). Two different nitrogen feeding strategies were applied in this study. For two cultures, a nitrogen-free feeding solution was implemented for promoting nitrogen starvation. Once the starvation occurred in the bioreactor (highlighted by biosensor activation and confirmed by analytical technique), a solution supplemented with nitrogen (4.5 M) was used until reaching a nitrogen concentration equivalent to the initial concentration. Finally, the nitrogen-free solution was implemented again.

A specific nitrogen feeding strategy was applied in a third fermentation, using the *glnAp*-based biosensor as a process control tool: the nitrogen-free feeding solution was used all along the process and ad-hoc additions of nitrogen solution were performed based on *glnAp* biosensor activity (see Section 2.8.2 for more details).

2.8 | Automated analysis of microbial population based on FCM

2.8.1 | FCM analysis

FCM analyses were performed directly after sampling (to avoid population evolution) using an Attune NxT cytometer (Thermo Fisher Scientific) equipped with a 50 mW Blue Laser (488 nm). Before analysis, the microbial biomass concentration in the sample was adjusted to reach approximately 5.0×10^6 cells/mL by dilution with NaCl 0.9% (w/v). Forward light scatter (FSC) and Side light scatter (SSC) signals were collected with a 488/10 bandpass filter, and green fluorescence (BL1 channel) was collected using a 530/30 bandpass filter. Photomultiplier voltages were set at 380, 320, and 510 V for, respectively, FSC, SSC, and BL1 channels. During sample analysis, a threshold was implemented based on both SSC and FSC signals to

only consider microbial cells: events with an SSC and/or FSC signals inferior to, respectively, 800 and 100 were not considered. For each sample run, data for 40,000 cells were collected with a flow rate of 12.5 μ L/min.

2.8.2 | FCMinterface

The general workflow for single-cell GFP analysis, data treatment, and retro-control feeding are illustrated in Figure 4a. The interfacing system between the bioreactor and the flow cytometer (Thermo Fischer Attune NxT) was adapted from the system initially developed by Brognaux et al. (2013) and further improved by Sassi et al. (2019). FCM analyses were performed according to the same protocol as for the offline analyses. The raw data were then extracted from the Attune software (Thermo Fisher Scientific) and loaded into GNU Octave software (<http://www.octave.org>) (Eaton, 2002) with the help of the *fca_readfsc* function (available on Matlab central at <http://www.mathworks.com/matlabcentral/fileexchange/9608-fcs-data-reader>) for data treatment. To maintain a cell concentration of approximately 5.0×10^6 cells/mL for the FCM analysis, the adequate dilution factor to apply to raw sample was determined before every analysis sequence and the samples were automatically diluted using NaCl 0.9% (w/v). The appropriate dilution factor is determined based on the cell concentration measured for the previous FCM analysis.

2.9 | Metabolite analysis

Extracellular glucose and ammonium concentrations were determined using colorimetric enzymatic tests (kit Ref 984304 and Ref 984320, respectively) implemented on a Gallery system (Thermo Fisher Scientific). Standard solutions were used for the determination of calibration curves. Culture media supplemented with defined concentrations of glucose and ammonium were used to validate the recovery level of the method and the absence of interference.

3 | RESULTS

3.1 | The *glnAp*-based biosensor is an effective sensor of nitrogen limitation

A genetically encoded biosensor was designed for monitoring nitrogen limitation in *E. coli* cultures. This biosensor is based on the *glnAp*-based promoter of *E. coli* as a sensing/input module, whose activation by ammonium limitation triggers the production of GFP (Figure 1a). In such a basic configuration, however, the biosensor is expected to be poorly dynamic, because GFP is highly stable (Andersen et al., 1998). Accordingly, preliminary evaluations (not shown) confirmed that after experiencing a first nitrogen starvation event, the cells remain fluorescent even when additional ammonium is provided, complicating the detection of multiple starvation events

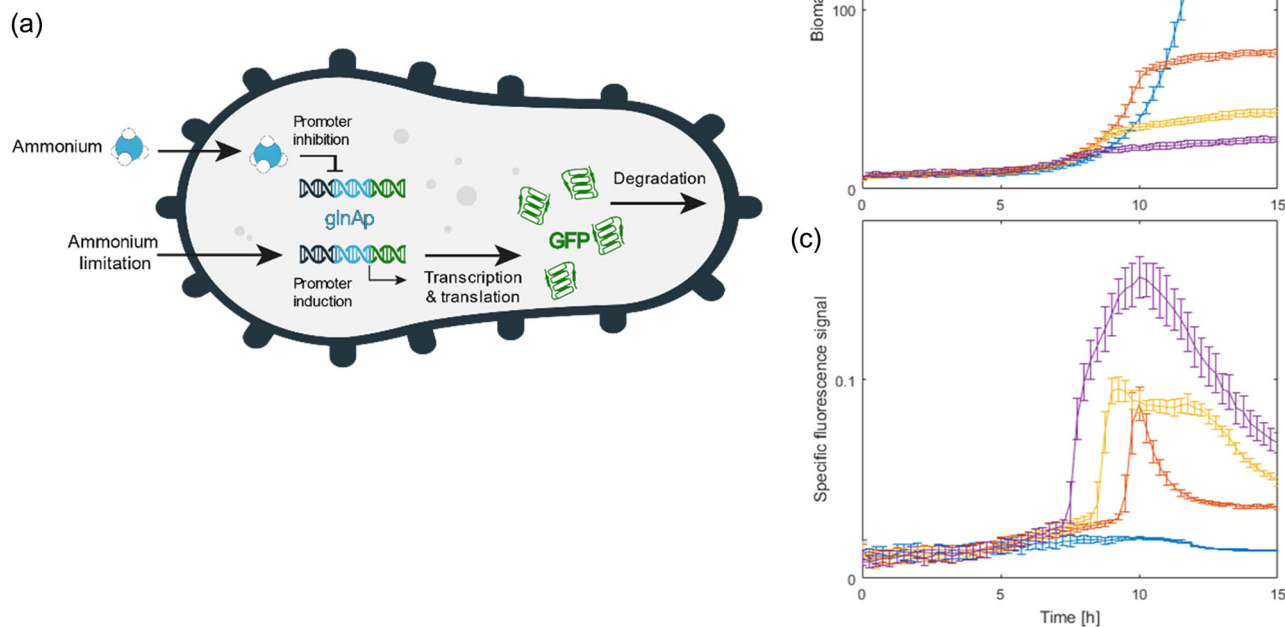


FIGURE 1 Validation of the *glnAp*-GFP-ASV biosensor functionality. (a) Schematic representation of the activation mechanism of the *glnAp*-GFP-ASV biosensor. (b, c) Evolution of the biomass and the specific fluorescence signal during Biolector cultivation for different initial ammonium concentrations (as indicated on the graph).

in the same culture. To improve the dynamics of the *glnAp*-based biosensor, a degradation tag (ASV tag; Andersen et al., 1998) was, therefore, added to the C-terminus of the protein.

To validate the functionality of the *glnAp*-GFP-ASV biosensor, we first evaluated its ability to detect a single nitrogen starvation event at the population level. Multiple parallel batch fermentations of *E. coli* BLR (DE3) carrying the biosensor were performed in a Biolector device (48-well plates), using CDM with a range of initial ammonium concentrations. The fluorescence and biomass concentration of each culture were monitored on-line (Figure 1b,c). Whereas the specific fluorescence signal (i.e., total fluorescence of the population divided by the biomass concentration) remained stable in cultures with excess initial ammonium concentration (56 mM), a sudden increase in specific fluorescence was observed with limiting NH_4Cl supply (2.2, 5.6, and 11.2 mM), coincident with a cessation of growth. As expected, this increase in fluorescence was detected earlier in cultures with the lowest ammonium concentration.

After the sharp initial increase, GFP fluorescence decreased progressively. This decrease cannot be attributed to growth-associated dilution of the GFP present in the cells, since no significant growth was observed after fluorescence increase. It can be more plausibly attributed to active degradation of GFP following targeting to the Clp protease machinery through its C-terminal extension. The difference in the amplitude of the biosensor response at different

initial ammonia concentrations most likely reflects differences in the metabolic state of the cells at the time of N starvation (for instance, specific nitrogen concentration available for GFP synthesis or activity of the ATP-dependent Clp proteolytic system for GFP-ASV degradation). Altogether, these results validate the functionality of the *glnAp*-GFP-ASV as a sensor of nitrogen starvation.

For further validation, we used microfluidics for characterizing the activation/deactivation of the of the *glnAp*-GFP-ASV biosensor. Briefly, cells were cultivated in two-dimensional microfluidic chambers in perfusion mode, allowing the continuous renewal of the cellular microenvironment and the decoupling between cellular physiology and the extracellular environment. Additionally, the system allows to shift tightly between two different environmental conditions, that is, in our case between the cultivation medium with and without nitrogen (Figure 2a).

We followed different cultivation chambers for growth (Figure 2b) and GFP fluorescence (Figure 2c). Upon switching to nitrogen-depleted conditions (i.e., after 3.3 h of cultivation), cells quickly expressed GFP. Then, the GFP signal dropped quickly due to the degradation tag. Interestingly, we observed the presence of GFP-positive cells after switching back to the cultivation conditions with nitrogen (Figure 2d). The movies (Supporting Information movies) pointed out that these cells were larger in size and were unable to grow after the nitrogen shift, even when the

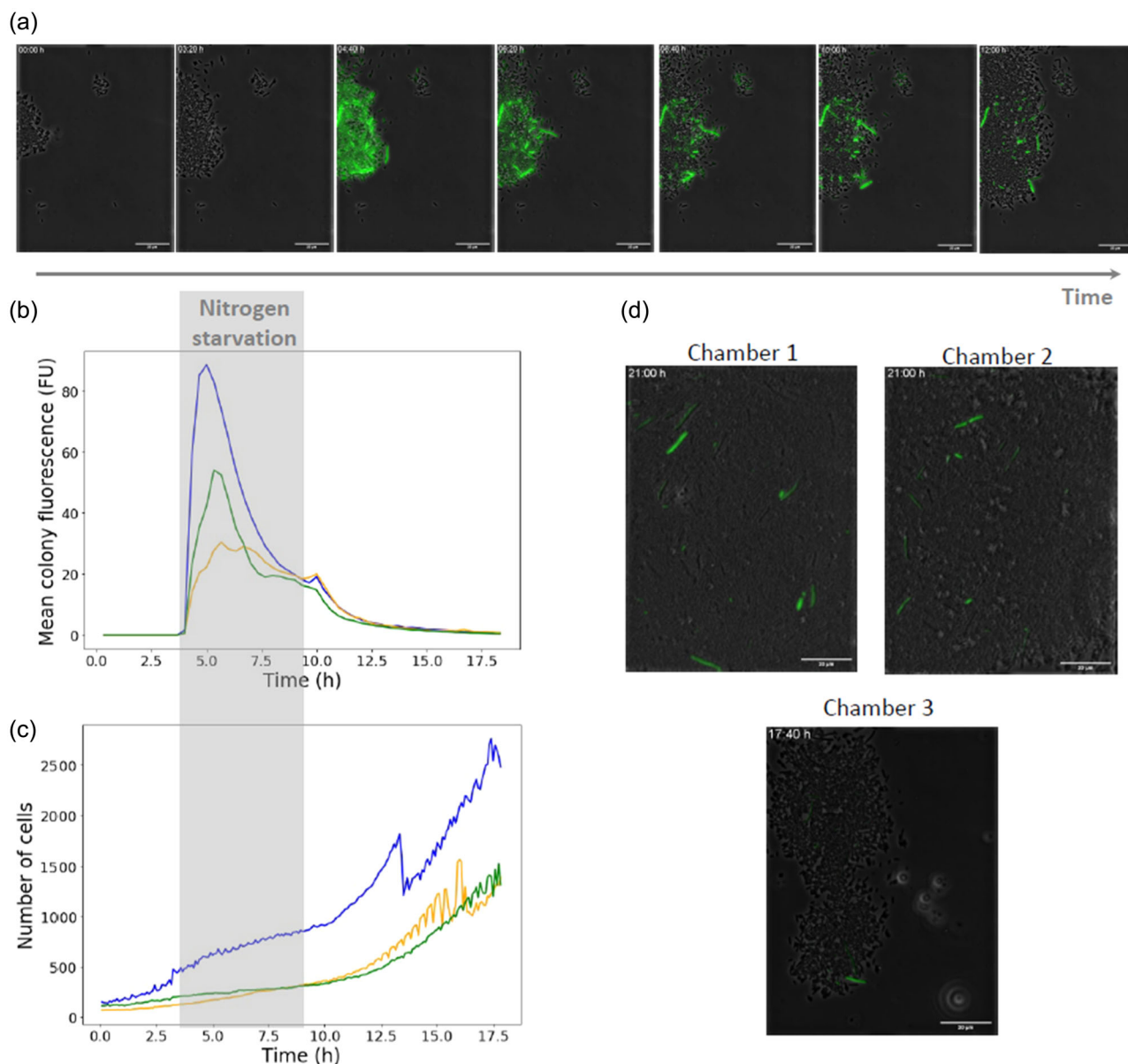


FIGURE 2 Characterization of the the *glnAp*-GFP-ASV biosensor in microfluidics cultivation device. (a) Snapshots taken from one representative cultivation chamber (three chambers have been followed, on three independent feeding lines). (b) Time evolution of the global GFP fluorescence in three different cultivation chambers. (c) Time evolution of the number of cells in three different cultivation chambers. (d) Snapshots of the cultivation chamber well after the nitrogen depletion stress. Large cells with GFP signals that are unable to grow are clearly visible on the pictures (full movies are provided as Supporting Information).

cultivation conditions went back to normal. This type of observation has been previously made for destabilized variant of GFP when *E. coli* was cultivated under nutrient-depleted conditions (Baert et al., 2015; Brognaux et al., 2013). Analyses pointed out that some cells exposed to nutrient starvation exhibited depletion in ATP necessary for the activation of the ClpXP proteases involved in the active degradation of the GFP-tagged variants (Brognaux et al., 2013). In the context of this study, this effect allows for the easy detection of cells exhibiting growth defect upon exposure to nitrogen depletion, further validating the usefulness of the *glnAp*-GFP-ASV biosensor.

3.2 | The *glnAp*-based biosensor captures the dynamics of nitrogen starvation in fed-batch cultivation at both the population and single-cell levels

Fed-batch fermentations in 2 L DasGip and 20 L bioreactors were performed to validate the biosensor functionality in conditions that are more similar to effective process conditions (Sections 2.6 and 2.7). The evolution of biomass concentration, nitrogen concentration, and green fluorescence signal are shown at Figure 3a–c for a representative cultivation in 2 L DasGip bioreactor and in Supporting

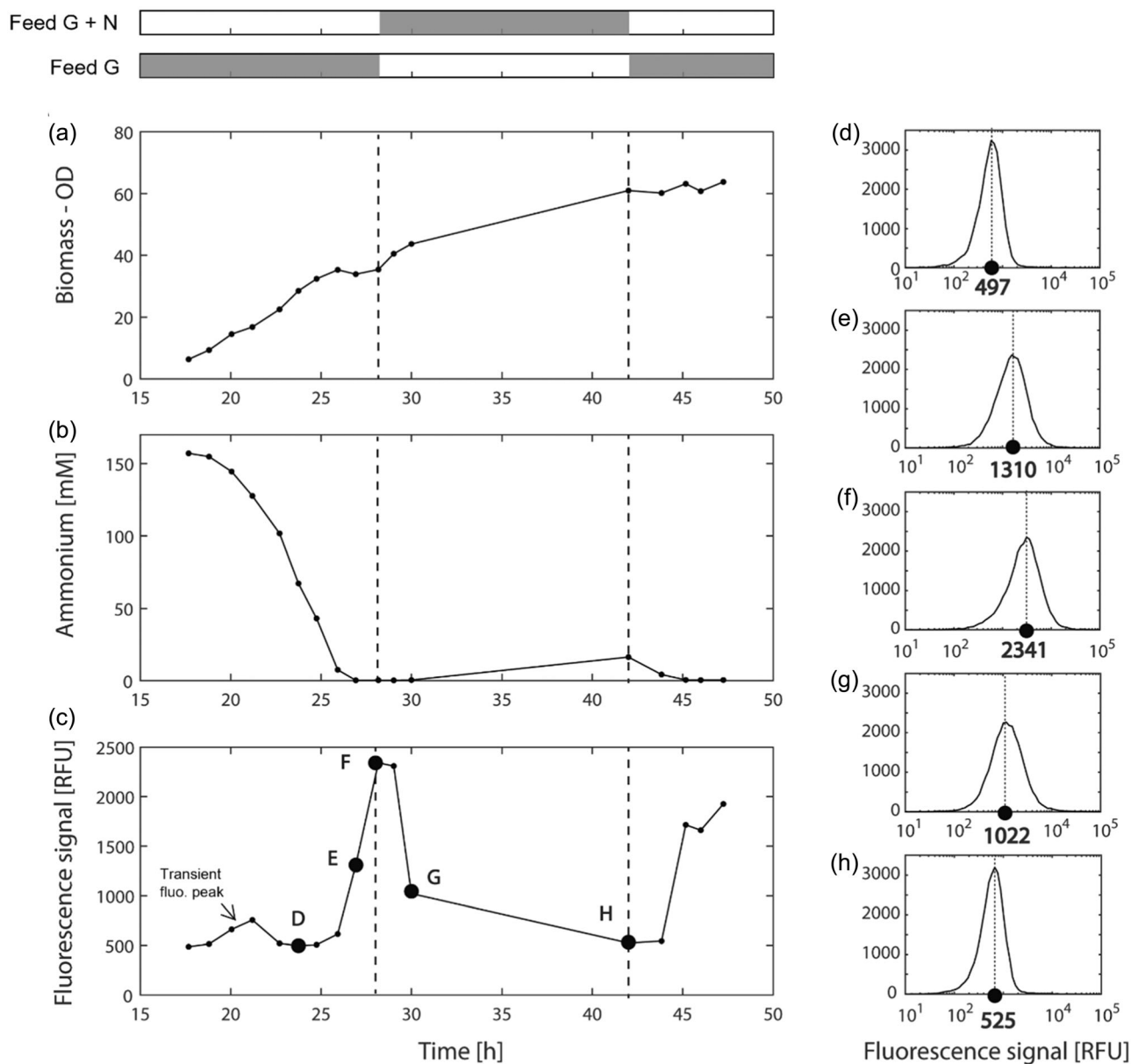


FIGURE 3 Validation of the *glnAp*-based biosensor in 2L DasGip fed-batch cultivations. Evolution of the biomass (a), the nitrogen concentration (b) and the fluorescence (c) in the culture medium during 2L DasGip bioreactor fed-batch cultivation. The dashed lines in (a–c) represent changes in feed composition. The two banners on the top of the figure indicate in black when the addition of solutions containing glucose and ammonium (Feed G + N) or glucose only (Feed G) are performed. The green fluorescence signal presented in panel (c) is the median value calculated for each sample of 40,000 cells: the associated histograms of the signal intensity at single-cell level are presented in (d–h) for five samples.

Information S1: Figure 1 for two 20-L fed-batch cultivations. The values of these three parameters measured during the 2L DasGip bioreactor cultivation are also shown in Table 1.

In contrast to the multiwell plate cultivations, the green fluorescence signal was measured at the single-cell level (off-line FCM analysis) and further averaged over thousands of cells: the reported signal corresponds to the median value of the fluorescence measured for at least 40,000 cells (see Section 2.8 for more details). The distribution of green fluorescence was found to be unimodal throughout cultivation (Figure 3d–h—unimodal distribution was

observed for all the collected samples, data not shown), denoting homogeneous activation of the *glnAp*-based biosensor upon ammonium depletion. In these conditions at least, the biosensor activity can thus be described using simple descriptive statistics such as the median of the fluorescence signal.

The *glnAp*-based biosensor was found to be activated when ammonia concentration dropped below 5–7.5 mM at both the 2 and 20-L scales (Figure 3b,c). Importantly, the biosensor demonstrated a dynamic behavior with respect to nitrogen availability: following a first nitrogen depletion event, the fluorescence signal rapidly

TABLE 1 Validation of the *glnAp*-based biosensor in 2 L DasGip fed-batch cultivations.

Flow cytometry histograms	Culture age (h)	Ammonium (mM)	Fluorescence signal (RFU)	Biomass –OD
-	17.7	157	487	4.34
-	18.8	155	515	5.16
-	20.1	144	662	6.95
-	21.2	128	757	10.2
-	22.7	102	521	25.4
D	23.8	67.3	497	21.9
-	24.8	43.1	507	26.3
-	25.9	7.56	615	31.8
E	26.9	0.277	1310	30.1
F	28.2	0.361	2341	30.4
-	29.0	0.262	2309	35.7
G	30.0	0.467	1022	38.0
H	42.0	16.3	525	60.5
-	43.8	4.27	544	57.2
-	45.2	0.543	1714	60.0
-	46.0	0.423	1660	57.0
-	47.3	0.509	1925	57.2

Note: Values measured for the biomass (OD 650 nm), the ammonium concentration (mM), and the fluorescence in the culture medium during 2 L DasGip bioreactor fed-batch cultivation. The green fluorescence values presented in this table are the median values calculated for each sample of 40,000 cells. During the cultivation, feed composition was changed. After 28.2 h of culture, a switch was made from a feed without nitrogen to a feed with nitrogen. Finally, after 42 h of culture, feed without nitrogen was used back in replacement of feed with nitrogen. Cross-references to the flow cytometry histograms presented in Figure 3 are made in the first column.

decreased when additional ammonia was supplied, and the biosensor could be reactivated by further nitrogen limitation events. Interestingly, the biosensor signal was reduced to a large extent after switching from a feeding solution without nitrogen to a feeding solution with nitrogen (Figure 3f,g) even if the extracellular ammonium concentration did not significantly increase (Figure 3c and Table 1). The ammonium addition going along with the feeding solution addition defined by the DO-stat strategy did not reflect in an increase of the extracellular ammonia concentration. Most of the continuously but smoothly added nitrogen was directly consumed by the growing cells. After 14 h of feeding with the solution containing ammonium, the accumulation of ammonium in the extracellular environment was equal to 16.3 mM. At this time (Figure 3h), the cell population almost retrieved the exact same shape than before nitrogen depletion (Figure 3d). Finally, after switching back to a feeding solution without nitrogen for only 3 h, a new increase of the biosensor signal was observed. Extracellular

ammonium concentrations close to 0 were measured at the moment of biosensor reactivation. It appears that in such fed-batch high cell density culture conditions, it is difficult to effectively assess the correlation between nitrogen availability and biosensor activation/deactivation. However, such a correlation has been proven with microfluidics cultivations (see Section 3.1).

It should be noted, that in all three experiments, a transient fluorescence increase was observed during the batch phase, when ammonia supply was still abundant (highlighted by an arrow at Figure 3c and Supporting Information S1: Figure 1). A possible hypothesis for this transient activation of the *glnAp*-based biosensor is the accumulation of cAMP at the end of the batch phase (Lin et al., 2004). The *glnA* gene has two promoter sequences, *glnAp1* (σ^{70}) and *glnAp2* (σ^{54}), both regulated by the CRP-cAMP complex (i.e., complex formed when the cAMP receptor protein binds with CRP), and *glnAp1* has been demonstrated to be activated by CRP-cAMP (Merrick & Edwards, 1995).

Thus, except for the initial transient activation in batch phase, the *glnAp*-based biosensor was found to efficiently report on the nitrogen supply status, in a dynamic fashion. This observation, combined with the observed capacity of the biosensor to activate before complete ammonia depletion, indicates that it could be used as an actuator for on-demand nitrogen feeding.

3.3 | Using *glnAp*-based biosensor for closed-loop fractionated feeding control

In typical industrial *E. coli* cultivation processes, the carbon source (glucose) is most often delivered according to the principle of exponential growth while the nitrogen needs are defined based on a priori ratio with respect to the provided carbon source (Waites et al., 2013). This strategy presents a high risk to over or undersupply nitrogen during the fermentation and, therefore, might not be optimal. To overcome this risk, we developed a closed-loop feeding strategy for supplying ammonia to the cultures whenever the nitrogen concentration becomes limiting, as sensed intracellularly.

Our strategy was developed in a 20-L bioreactor, and uses an interfacing system between the bioreactor and a flow cytometer (Section 2.8.2) for online monitoring of the *glnAp*-GFP-ASV biosensor signal (Figure 4a). The monitoring frequency is dependent on the cell concentration in the bioreactor: at the early stages of the culture, the fluorescence signal is monitored every 30 min whereas at higher cell densities, the signal of the biosensor can be monitored every 6 min (see Supporting Information S1: Table 2 for the exact sampling times). The median fluorescence signal is then used as the actuator of the fractionated nitrogen feeding. Practically, 0.5 mol NH₄Cl are added whenever the following conditions are fulfilled: (1) no NH₄Cl addition has been performed at the previous sampling point; (2) the slope of fluorescence change between the current and previous sampling points is greater than 400 RFU h⁻¹; and (3) the median fluorescence signal at the current sampling time is greater than 600 RFU. This last condition ensures that nitrogen feeding is not applied in response to

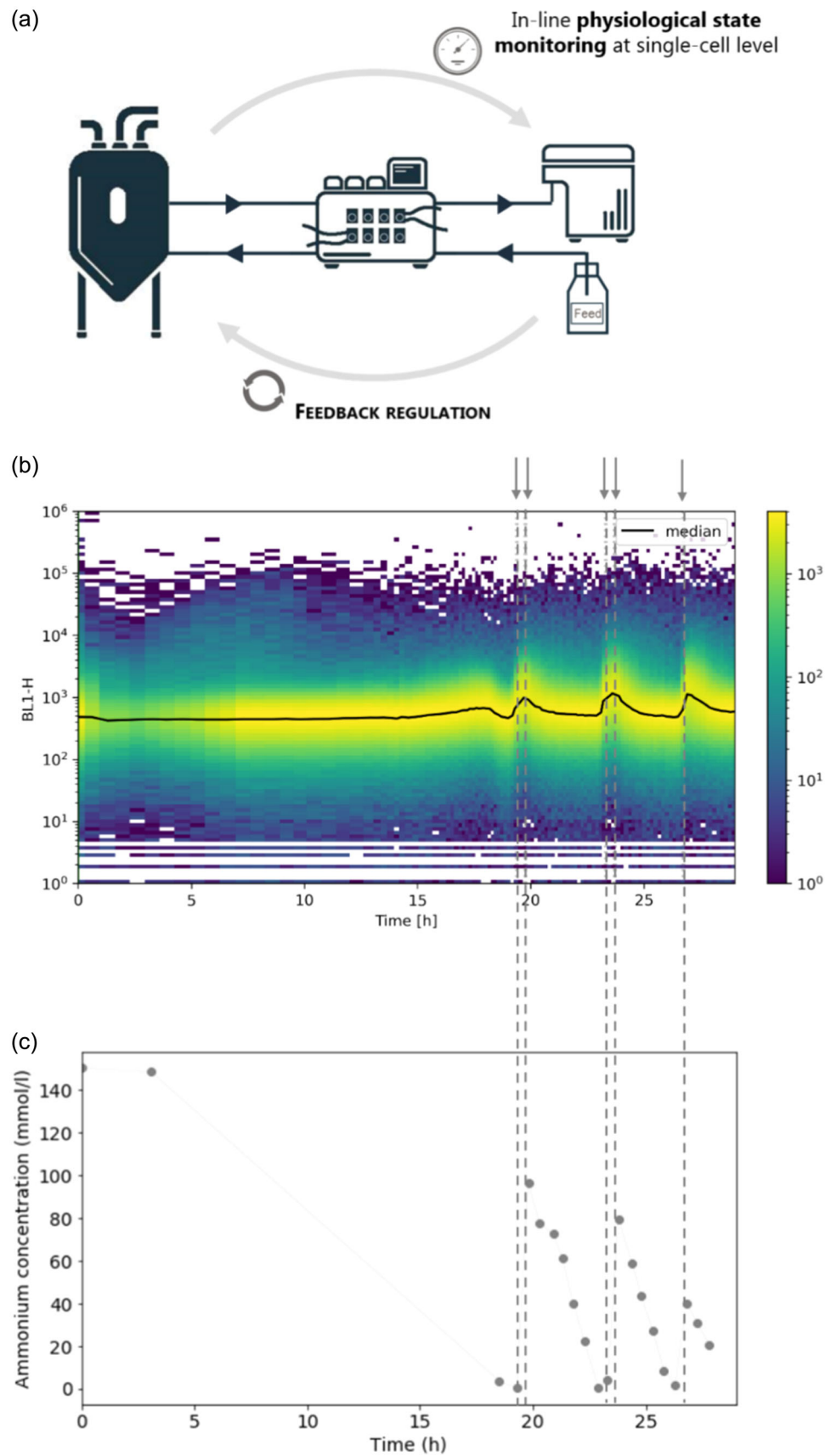


FIGURE 4 (See caption on next page).

low-amplitude fluorescence peaks such as the transient peak observed in the batch phase of the previous bioreactor experiments (Figures 3 and 4b).

The evolution of the fluorescence signal for this closed-loop fractionated nitrogen-fed *E. coli* culture is shown in Figure 4b. To validate that the nitrogen injections were performed at the right time (i.e., when cells were actually facing nitrogen limitation), the ammonium concentration in the culture medium was determined off-line at selected times during the fermentation. The results of these measurements are also presented in Figure 4c. The first nitrogen addition occurred 1 h after the start of glucose feeding (i.e., 19.3 h of fermentation). A total of five injections were performed between 20 and 40 h of fermentation (i.e., 19.3, 23.2, 26.7, 29.3, and 39 h). Four of these five injections were performed in tandem, that is, at two successive sampling time intervals (Figure 4b). The reason is that, despite nitrogen starvation was overcome with the first injection, the fluorescence signal resulting from the biosensor activity kept increasing, resulting in a second unnecessary injection. These results indicate that a delay exists between nitrogen addition and the observation of the biosensor "inactivation." To avoid such over-feeding in the future, this delay should be taken into account for the definition of the regulation parameters.

The molecular mechanisms responsible for the expression and the degradation of the reporter protein might be an explanation for the observation of such lag phases; as translation of the coding sequence, transcription of the messenger RNA, maturation of the GFP, and degradation of the protein are not instantaneous mechanisms.

4 | DISCUSSION

The biopharmaceutical industry is driven by delivering on the promise of real-time drug release, currently expected to be achievable through the implementation of smart manufacturing (i.e., Industry 4.0) (Narayanan et al., 2020). In this context, advanced process control strategies are expected to play a major role as they would allow the real-time adjustment of the process trajectories such that process productivity and quality of the product can be guaranteed. To date, most of the bioprocess control strategies rely on the monitoring of the concentrations of key compounds that drive cellular metabolism, for example with NIR, FTIR, or Raman (Buckley & Ryder, 2017; Guerra et al., 2019). However, monitoring of these environmental parameters does not enable tracking the metabolic

state of the cell population. This prevents the maintenance of an optimal environment to reach the desired bioprocess performance along with critical drug quality attributes. In this context, innovative molecular and analytical tools are required to monitor physiological parameters at the single-cell level.

To this end, we used genetically encoded biosensors in combination with online flow cytometry to obtain a real-time "physiological fingerprint" of the population at the single-cell level. We designed, constructed, and evaluated a *glnAP*-based biosensor for the direct monitoring of nitrogen limitation. We further validated the biosensor functionality with multiple cultures at different scales (from microplate to 20-L bioreactor). We also developed a fully automated bioreactor-flow-cytometer interface enabling online monitoring of the microbial population. We showed that in the case of our process, the population can be efficiently described by only using simple descriptive statistical parameters such as the median or the average of the fluorescence signal measured for a set of cells.

Note that this conclusion might not be valid with another process or at greater scale, as, for example, the mixing efficiency could be reduced when scaling-up. Therefore, individual cells might face different environmental conditions (nitrogen gradient) and the population might become more heterogeneous from the biosensor activity perspective. Indeed, numerous studies have shown that a clonal population of microorganisms (i.e., population of microorganisms sharing the same genotype) can segregate into several subpopulations with different phenotypes (e.g., different recombinant protein productivity and/or production of protein with different quality attributes) due for instance to environmental pressures such as the substrate concentration surrounding the cells (Delvigne et al., 2014, 2015; Ryall et al., 2012). Especially, conditions such as high substrate concentration or starvation may cause the appearance of subpopulations of reduced production efficiency. Hence, such population heterogeneity is seen as a drawback in the context of bioprocess manufacturing. Importantly, the tools developed in the present study could be used for monitoring and controlling such phenotypic heterogeneity, to improve bioprocess robustness and reproducibility (Delvigne & Goffin, 2014).

Finally, we experimentally validated the proposed bioprocess control approach with the implementation of a feedback control loop manipulating the nitrogen feeding. We demonstrated that *glnAp*-based biosensor could effectively be used as an actuator of fractionated nitrogen feeding. However, due to the sample preparation, the interval between measurements, and analysis time, there was a delay on the nitrogen addition, hence the cells encountered

FIGURE 4 *glnAp*-based biosensor is used to control nitrogen feeding. (a) Schematic representation of the interfacing between the bioreactor and the flow cytometer that is used to control the ammonium feeding during the fed-batch cultivation. (b) Fed-batch experiment in 20 L bioreactor with ammonia pulse at 19.3, 23.2, 26.7, 29.3, and 39 h (0.5 mole NH_4Cl added at each injection, pulses are denoted by the gray dotted vertical lines). Automated flow cytometry (FC) data are displayed as a scatter plot time profile of the BL1-H channel scaling with GFP accumulation inside cells. The scale bar represents the density of cells exhibiting a given fluorescence intensity, as determined based on automated FC. (c) Time evolution of the ammonium concentration during the cultivation, as well as the median fluorescence obtained based on automated FC.

very low nitrogen concentrations before feeding. In the future, a predictive control strategy could be implemented to prevent any low nitrogen condition. Overall, the approach holds great promise for the future of bioprocess control but also Process Analytical Tools (PAT 2.0) in the biopharmaceutical industry. Indeed, the proposed methodology allows to communicate in real time with cell population and react accordingly, that is, in our case, by adding the nutrients needed for growth. However, considering the developments made at the level of signal multiplexing for fluorescent biosensors (Anzalone et al., 2021; Heins et al., 2020), this approach could be extended in the future to the detection of different kinds of nutrients and also to the eventual metabolic burden exerted on cells (Ceroni et al., 2018). In this case, more complex biosensor responses have to be expected. The *glnAP*-based biosensor did not lead to the observation of complex behavior at the level of the cell population, such as bimodality distribution of the response. At this stage, we can assess that, based on the reactive FCM protocol proposed (Bertaux et al., 2022; Nguyen et al., 2021), the methodology presented in this work could be easily extended to the control of more complex cellular responses.

Despite the many advantages in terms of process control, the implementation of biosensors in the manufacturing environment might be challenging. The modification of the strain DNA backbone by incorporation of the specific biosensor sequence and subsequent expression of an additional recombinant protein (i.e., *gfp* as reporter protein) might form an issue for regulatory approval. Nevertheless, this work showed that biosensors form a valuable tool toward an in-depth process understanding. Acquiring such detailed knowledge leads in itself to a high-quality process by design.

Biosensors data have also the potential for improving the training of parametric probes models (e.g., RAMAN spectroscopy), as well as soft sensors.

AUTHOR CONTRIBUTIONS

Romain Kinet: Design of the study; study development; data acquisition; data analysis and interpretation. **Anne Richelle:** Study development; data analysis and interpretation. **Michaël Colle:** Study development; acquisition of data; data analysis and interpretation. **Didier Demaegd:** Design of the study; study development; data acquisition; data analysis and interpretation. **Moritz van Stosch:** Study development; **Matthew Sanders:** Design of the study. **Hannah Sehart:** Study development; acquisition of data; data analysis and interpretation. **Franck Delvigne:** Study development; data analysis and interpretation. **Philippe Goffin:** Design of the study; study development; data analysis and interpretation. All authors were involved in the development of the manuscript and approved the final version.

ACKNOWLEDGMENTS

This work was sponsored by GlaxoSmithKline Biologicals SA. R. K., D. D., M. C., A. R., M. v. S., M. S. are, or were at the time of the study employees of the GSK group of companies. R. K., D. D., P. G., and F.

D. were supported by a Wagralim-Biowin grant (SingleCells project n° 7273).

DATA AVAILABILITY STATEMENT

The data that support the findings of this study are available from the corresponding author upon reasonable request.

ORCID

Romain Kinet  <http://orcid.org/0009-0000-7179-8724>

Franck Delvigne  <http://orcid.org/0000-0002-1679-1914>

REFERENCES

- Andersen, J. B., Sternberg, C., Poulsen, L. K., Bjørn, S. P., Givskov, M., & Molin, S. (1998). New unstable variants of green fluorescent protein for studies of transient gene expression in bacteria. *Applied and Environmental Microbiology*, 64(6), 2240–2246. <https://doi.org/10.1128/AEM.64.6.2240-2246.1998>
- Anzalone, A. V., Jimenez, M., & Cornish, V. W. (2021). FRAME-tags: Genetically encoded fluorescent markers for multiplexed barcoding and time-resolved tracking of live cells. *BioRxiv*. <https://doi.org/10.1101/2021.04.09.436507>
- Babaeipour, V., Shojaosadati, S. A., Robotjazi, S. M., Khalilzadeh, R., & Maghsoudi, N. (2007). Over-production of human interferon- γ by HCDC of recombinant *Escherichia coli*. *Process Biochemistry*, 42(1), 112–117. <https://doi.org/10.1016/j.procbio.2006.07.009>
- Baert, J., Kinet, R., Brognaux, A., Delepierre, A., Telek, S., Sørensen, S. J., Riber, L., Fickers, P., & Delvigne, F. (2015). Phenotypic variability in bioprocessing conditions can be tracked on the basis of on-line flow cytometry and fits to a scaling law. *Biotechnology Journal*, 10(8), 1316–1325. <https://doi.org/10.1002/biot.201400537>
- Benisch, M., Benzinger, D., Kumar, S., Hu, H., & Khammash, M. (2023). Optogenetic closed-loop feedback control of the unfolded protein response optimizes protein production. *Metabolic Engineering*, 77, 32–40. <https://doi.org/10.1016/j.ymben.2023.03.001>
- Bertaux, F., Sosa-Carrillo, S., Gross, V., Fraisse, A., Aditya, C., Furstenheim, M., & Batt, G. (2022). Enhancing bioreactor arrays for automated measurements and reactive control with ReacSight. *Nature Communications*, 13(1), 3363. <https://doi.org/10.1038/s41467-022-31033-9>
- Bhattacharya, S. K., & Dubey, A. K. (1997). High-Level expression of a heterologous gene in *Escherichia coli* in response to carbon-nitrogen source and C/N ratio in a batch bioreactor. *Biotechnology Progress*, 13(2), 151–155. <https://doi.org/10.1021/bp970007t>
- Brognaux, A., Han, S., Sørensen, S. J., Lebeau, F., Thonart, P., & Delvigne, F. (2013). A low-cost, multiplexable, automated flow cytometry procedure for the characterization of microbial stress dynamics in bioreactors. *Microbial Cell Factories*, 12(1), 100. <https://doi.org/10.1186/1475-2859-12-100>
- Brondyk, W. H. (2009). Chapter 11 selecting an appropriate method for expressing a recombinant protein. *Methods in Enzymology*, 463(C), 131–147. [https://doi.org/10.1016/S0076-6879\(09\)63011-1](https://doi.org/10.1016/S0076-6879(09)63011-1)
- Buckley, K., & Ryder, A. G. (2017). Applications of Raman spectroscopy in biopharmaceutical manufacturing: A short review. *Applied Spectroscopy*, 71(6), 1085–1116. <https://doi.org/10.1177/0003702817703270>
- Carrasco-López, C., García-Echauri, S. A., Kichuk, T., & Avalos, J. L. (2020). Optogenetics and biosensors set the stage for metabolic cybergenetics. *Current Opinion in Biotechnology*, 65, 296–309. <https://doi.org/10.1016/j.copbio.2020.07.012>
- Ceroni, F., Boo, A., Furini, S., Gorochowski, T. E., Borkowski, O., Ladak, Y. N., Awan, A. R., Gilbert, C., Stan, G.-B., & Ellis, T. (2018).

- Burden-driven feedback control of gene expression. *Nature Methods*, 15(5), 387–393. <https://doi.org/10.1038/nmeth.4635>
- Delvigne, F., Baert, J., Gofflot, S., Lejeune, A., Telek, S., Johanson, T., & Lantz, A. E. (2015). Dynamic single-cell analysis of *Saccharomyces cerevisiae* under process perturbation: Comparison of different methods for monitoring the intensity of population heterogeneity. *Journal of Chemical Technology & Biotechnology*, 90(2), 314–323. <https://doi.org/10.1002/jctb.4430>
- Delvigne, F., & Goffin, P. (2014). Microbial heterogeneity affects bioprocess robustness: Dynamic single-cell analysis contributes to understanding of microbial populations. *Biotechnology Journal*, 9(1), 61–72. <https://doi.org/10.1002/biot.201300119>
- Delvigne, F., & Martinez, J. A. (2023). Advances in automated and reactive flow cytometry for synthetic biotechnology. *Current Opinion in Biotechnology*, 83, 102974. <https://doi.org/10.1016/j.copbio.2023.102974>
- Delvigne, F., Zune, Q., Lara, A. R., Al-Soud, W., & Sørensen, S. J. (2014). Metabolic variability in bioprocessing: Implications of microbial phenotypic heterogeneity. *Trends in Biotechnology*, 32(12), 608–616. <https://doi.org/10.1016/j.tibtech.2014.10.002>
- Dietzsch, C., Spadiut, O., & Herwig, C. (2013). On-line multiple component analysis for efficient quantitative bioprocess development. *Journal of Biotechnology*, 163(4), 362–370. <https://doi.org/10.1016/j.jbiotec.2012.03.010>
- Eaton, J. W. (2002). *GNU octave manual*. Network Theory Limited.
- Esmonde-White, K. A., Cuellar, M., Uerpmann, C., Lenain, B., & Lewis, I. R. (2017). Raman spectroscopy as a process analytical technology for pharmaceutical manufacturing and bioprocessing. *Analytical and Bioanalytical Chemistry*, 409(3), 637–649. <https://doi.org/10.1007/s00216-016-9824-1>
- Goffin, P., & Dehottay, P. (2017). Complete genome sequence of *Escherichia coli* BLR(DE3), a recA-deficient derivative of *E. coli* BL21(DE3). *Genome Announcements*, 5(22), 4099–4100. <https://doi.org/10.1128/genomeA.00441-17>
- Guerra, A., von Stosch, M., & Glassey, J. (2019). Toward biotherapeutic product real-time quality monitoring. *Critical Reviews in Biotechnology*, 39(3), 289–305. <https://doi.org/10.1080/07388551.2018.1524362>
- Heins, A.-L., Reyelt, J., Schmidt, M., Kranz, H., & Weuster-Botz, D. (2020). Development and characterization of *Escherichia coli* triple reporter strains for investigation of population heterogeneity in bioprocesses. *Microbial Cell Factories*, 19(1), 14. <https://doi.org/10.1186/s12934-020-1283-x>
- Heins, A.-L., & Weuster-Botz, D. (2018). Population heterogeneity in microbial bioprocesses: Origin, analysis, mechanisms, and future perspectives. *Bioprocess and Biosystems Engineering*, 41(7), 889–916. <https://doi.org/10.1007/s00449-018-1922-3>
- Kumar, S., & Khammash, M. (2022). Platforms for optogenetic stimulation and feedback control. *Frontiers in Bioengineering and Biotechnology*, 10, 918917. <https://doi.org/10.3389/fbioe.2022.918917>
- Kumar, S., Rullan, M., & Khammash, M. (2021). Rapid prototyping and design of cybergenetic single-cell controllers. *Nature Communications*, 12(1), 5651. <https://doi.org/10.1038/s41467-021-25754-6>
- Lemoine, A., Delvigne, F., Bockisch, A., Neubauer, P., & Junne, S. (2017). Tools for the determination of population heterogeneity caused by inhomogeneous cultivation conditions. *Journal of Biotechnology*, 251, 84–93. <https://doi.org/10.1016/j.jbiotec.2017.03.020>
- Lin, H., Hoffmann, F., Rozkov, A., Enfors, S.-O., Rinas, U., & Neubauer, P. (2004). Change of extracellular cAMP concentration is a sensitive reporter for bacterial fitness in high-cell-density cultures of *Escherichia coli*. *Biotechnology and Bioengineering*, 87(5), 602–613. <https://doi.org/10.1002/bit.20152>
- Lv, P. J., Qiang, S., Liu, L., Hu, C. Y., & Meng, Y. H. (2020). Dissolved-oxygen feedback control fermentation for enhancing β -carotene in engineered *Yarrowia lipolytica*. *Scientific Reports*, 10(1), 17114. <https://doi.org/10.1038/s41598-020-74074-0>
- Mandenius, C.-F., & Gustavsson, R. (2016). Soft sensor design for bioreactor monitoring and control. In C.-F. Mandenius (Ed.), *Bioreactors* (pp. 391–420). <https://doi.org/10.1002/9783527683369.ch14>
- Merrick, M. J., & Edwards, R. A. (1995). Nitrogen control in bacteria. *Microbiological Reviews*, 59(4), 604–622.
- Narayanan, H., Luna, M. F., von Stosch, M., Cruz Bournazou, M. N., Polotti, G., Morbidelli, M., Butté, A., & Sokolov, M. (2020). Bioprocessing in the digital age: The role of process models. *Biotechnology Journal*, 15(1), 1900172. <https://doi.org/10.1002/biot.201900172>
- Nguyen, T. M., Telek, S., Zicler, A., Martinez, J. A., Zacchetti, B., Kopp, J., Slouka, C., Herwig, C., Grünberger, A., & Delvigne, F. (2021). Reducing phenotypic instabilities of a microbial population during continuous cultivation based on cell switching dynamics. *Biotechnology and Bioengineering*, 118(10), 3847–3859. <https://doi.org/10.1002/bit.27860>
- Polizzi, K. M., & Kontoravdi, C. (2015). Genetically-encoded biosensors for monitoring cellular stress in bioprocessing. *Current Opinion in Biotechnology*, 31, 50–56. <https://doi.org/10.1016/j.copbio.2014.07.011>
- Richelle, A., David, B., Demaegd, D., Dewerchin, M., Kinet, R., Morreale, A., Portela, R., Zune, Q., & von Stosch, M. (2020). Towards a widespread adoption of metabolic modeling tools in biopharmaceutical industry: A process systems biology engineering perspective. *NPJ Systems Biology and Applications*, 6(1), 6. <https://doi.org/10.1038/s41540-020-0127-y>
- Ryall, B., Eydallin, G., & Ferenci, T. (2012). Culture history and population heterogeneity as determinants of bacterial adaptation: The adaptomics of a single environmental transition. *Microbiology and Molecular Biology Reviews*, 76(3), 597–625. <https://doi.org/10.1128/MMBR.05028-11>
- Ryder, A. G. (2018). Cell culture media analysis using rapid spectroscopic methods. *Current Opinion in Chemical Engineering*, 22, 11–17. <https://doi.org/10.1016/j.coche.2018.08.008>
- Sassi, H., Nguyen, T. M., Telek, S., Gosset, G., Grünberger, A., & Delvigne, F. (2019). Segregostat: A novel concept to control phenotypic diversification dynamics on the example of gram-negative bacteria. *Microbial Biotechnology*, 12(5), 1064–1075. <https://doi.org/10.1111/1751-7915.13442>
- Seo, J. D., Jin, D., Chung, B. H., Hwang, Y. D., & Park, Y. H. (1992). Glucose-limited fed-batch culture of *Escherichia coli* for production of recombinant human interleukin-2 with the DO-stat method. *Journal of Fermentation and Bioengineering*, 74(3), 196–198. [https://doi.org/10.1016/0922-338X\(92\)90085-9](https://doi.org/10.1016/0922-338X(92)90085-9)
- Steel, H., Habgood, R., Kelly, C. L., & Papachristodoulou, A. (2020). In situ characterisation and manipulation of biological systems with Chi.Bio. *PLoS Biology*, 18(7), e3000794. <https://doi.org/10.1371/journal.pbio.3000794>
- Täuber, S., Golze, C., Ho, P., von Lieres, E., & Grünberger, A. (2020). dMSSC: A microfluidic platform for microbial single-cell cultivation of corynebacterium glutamicum under dynamic environmental medium conditions. *Lab on a Chip*, 20(23), 4442–4455. <https://doi.org/10.1039/d0lc00711k>
- Thomsson, E., Gustafsson, L., & Larsson, C. (2005). Starvation response of *Saccharomyces cerevisiae* grown in anaerobic nitrogen- or carbon-limited chemostat cultures. *Applied and Environmental Microbiology*, 71(6), 3007–3013. <https://doi.org/10.1128/AEM.71.6.3007-3013.2005>
- Tibocha-Bonilla, J. D., Kumar, M., Richelle, A., Godoy-Silva, R. D., Zengler, K., & Zuñiga, C. (2020). Dynamic resource allocation drives growth under nitrogen starvation in eukaryotes. *NPJ Systems Biology and Applications*, 6(1), 14. <https://doi.org/10.1038/s41540-020-0135-y>

- Waites, M. J., Morgan, N. L., Rockey, J. S., & Higton, G. (2013). *Industrial microbiology: An introduction*. Wiley. <https://books.google.be/books?id=fjNIDAAAQBAJ>
- Wang, Y., Wu, S.-L., Hancock, W. S., Trala, R., Kessler, M., Taylor, A. H., Patel, P. S., & Aon, J. C. (2005). Proteomic profiling of *Escherichia coli* proteins under high cell density fed-batch cultivation with overexpression of phosphogluconolactonase. *Biotechnology Progress*, 21(5), 1401–1411. <https://doi.org/10.1021/bp050048m>
- Wong, B. G., Mancuso, C. P., Kiriakov, S., Bashor, C. J., & Khalil, A. S. (2018). Precise, automated control of conditions for high-throughput growth of yeast and bacteria with eVOLVER. *Nature Biotechnology*, 36(7), 614–623. <https://doi.org/10.1038/nbt.4151>
- Xu, Y., Wang, Y., Yang, Y., & Zhou, D. (2016). The role of starvation in biomass harvesting and lipid accumulation: Co-culture of microalgae–bacteria in synthetic wastewater. *Environmental Progress & Sustainable Energy*, 35(1), 103–109. <https://doi.org/10.1002/ep.12206>
- Zeng, W., Guo, L., Xu, S., Chen, J., & Zhou, J. (2020). High-throughput screening technology in industrial biotechnology. *Trends in Biotechnology*, 38(8), 888–906. <https://doi.org/10.1016/j.tibtech.2020.01.001>

SUPPORTING INFORMATION

Additional supporting information can be found online in the Supporting Information section at the end of this article.

How to cite this article: Kinet, R., Richelle, A., Colle, M., Demaegd, D., von Stosch, M., Sanders, M., Sehr, H., Delvigne, F., & Goffin, P. (2024). Giving the cells what they need when they need it: Biosensor-based feeding control. *Biotechnology and Bioengineering*, 1–13. <https://doi.org/10.1002/bit.28657>